KINETIC, ISOTHERM AND EQUILIBRIUM STUDY OF ADSORPTION OF HYDROGEN SULFIDE FROM WASTEWATER USING MODIFIED EGGSHELLS

OMAR ABED HABEEB[1], RAMESH KANTHASAMY[1]*, GOMAA ABDELGAWAD MOHAMMED ALI[2,3], ROSLI BIN MOHD. YUNUS[1] AND OLUSEGUN ABAYOMI OLALERE[1]

[1]Faculty of Chemical & Natural Resources Engineering,
[2]Faculty of Industrial Sciences & Technology,
Universiti Malaysia Pahang, 26300 Gambang, Pahang, Malaysia.
[3]Chemistry Department, Faculty of Science, Al–Azhar University, Assiut, 71524, Egypt.

**Corresponding author: ramesh@ump.edu.my*

(Received: 22nd June 2016; Accepted: 14th Nov. 2016; Published online: 30th May 2017)

ABSTRACT: The studies of adsorption equilibrium isotherms and the kinetics of hydrogen sulfide–water systems on calcite–based adsorbents prepared from eggshells were undertaken. The effects of operating variables, such as contact time and initial concentration, on the adsorption capacity of hydrogen sulfide are investigated. The modified eggshells are characterized using different analytical approaches such as Scanning Electron Microscopy (SEM) and Fourier Transform Infrared (FTIR). The batch mode adsorption process is performed at optimum removal conditions: dosage of 1 g/L, pH level of pH 6, agitation speed of 150 rpm, and contact time of 14 h for adsorbing hydrogen sulfide with an initial concentration of 100–500 mg/L. In the current study, the Langmuir, Freundlich, Temkin, and Dubinin models are used to predict the adsorption isotherms. Our equilibrium data for hydrogen sulfide adsorption agrees well with those of the Langmuir equation. The maximum monolayer adsorption capacity is 150.07 mg/g. Moreover, the kinetics of H_2S adsorption using the modified calcite of eggshells follows a pseudo–second–order model. From the current work, it has been found that the calcite eggshells are a suitable adsorbent for H_2S containing wastewater. Most importantly, chicken eggshells are waste products that are vastly available; hence, they could serve as a practical means for H_2S adsorption.

ABSTRAK: Kajian keseimbangan isoterma penjerapan dan kinetik sistem air– hidrogen sulfida terhadap penjerap berasaskan calcite yang disediakan daripada kulit telur telah dijalankan. Kesan pembolehubah operasi seperti masa jerapan dan kepekatan awal pada kapasiti penjerapan hidrogen sulfida disiasat. Kulit telur yang telah diubahsuai dianalisa menggunakan cara analisis yang berbeza seperti Scanning Electron Microscopy (SEM) dan Fourier Transform Infrared (FTIR). Proses penjerapan untuk mod batch dilakukan pada keadaan penyingkiran optimum: dos 1 g/L, tahap pH pH 6, kelajuan pergolakan 150 rpm dan masa jerapan 14 jam untuk menjerap hidrogen sulfida dengan kepekatan awal 100–500 mg/L. Dalam kajian semasa, model Langmuir, Freundlich, Temkin dan Dubinin digunakan untuk meramalkan isoterma penjerapan. Data keseimbangan yang diperoleh untuk penjerapan hidrogen sulfida mengikut baik persamaan Langmuir. Kapasiti maksimum penjerapan monolayer adalah 150.07 mg/g. Selain itu, kinetik penjerapan H_2S menggunakan kalsit kulit telur yang diubah suai didapati mengikut model pseudo–tertib kedua. Dari kerja semasa, ia telah mendapati bahawa calcite daripada kulit telur adalah penjerap sesuai untuk H_2S yang mengandungi air sisa. Perkara yang paling penting, kulit telur ayam boleh didapati secara meluas; oleh itu, ia boleh dijalankan secara praktikal sebagai medium untuk penjerapan H_2S.

KEYWORDS: *adsorbents; hydrogen sulfide; chicken eggshells; kinetic; isotherm*

1. INTRODUCTION

Hydrogen sulfide (H_2S) is an exceptionally deadly and damaging substance that is broadly delivered as a by–product in many industries. H_2S can bring about wellbeing issues, for example, coma, irritation of eyes, and respiratory system irritation. Excess exposure to H_2S might cause both chronic and acute ramifications [1, 2]. A concentration of H_2S equivalent to 500 – 1000 ppm or more, can threaten human life and lead to imminent impairment on the human physique [3]. Therefore, the Occupational Safety and Health Administration (OSHA) has regulated the exposure limit to 20 ppm for the general industry. Moreover, the neural system and major organs, such as the liver and the kidneys, are the main target of H_2S [4, 5]. On the other hand, another risk associated with H_2S in the natural environment is the threat of acid rain, which is precipitated through its oxidation into water–soluble sulfuric acid (4–6 g/L) [6]. In a solution, H_2S exists in three forms, i.e. H_2S, bisulfide (HS^-) and sulfide (S^{2-}) [7]. Moreover, H_2S safety problems posed by its highly flammable nature as well as economic problems arising from corrosion of metals (even in the low level of H_2S) [8]. In addition, H_2S is a corrosive medium for wastewater pipelines [9]. Another negative impact is that H_2S is one of the main poisons for many industry catalysts. In addition, it is a destructive gas to pipelines and equipment [10].

On a very frequent basis, adsorption is employed in wastewater treatment to remove toxic materials from industrial effluents [11]. Wastewater (e.g. from petroleum refinery plants) contains a huge amount of organic and inorganic toxic materials, such as H_2S. Most of the waste water from petroleum refineries is treated using chemical substances to remove toxic pollutants such H_2S. These chemicals consist of strong oxidants such as peroxide (H_2O_2), sodium hypochlorite (NaOCl), and sodium hydroxide (NaOH) [12]. The shortcoming of hydrogen peroxide, sodium/calcium hypochlorite and ferrous/ferric salts on dissociation of H_2S in wastewater have been investigated by Abdullah [12] who notes that strong oxidants would increase the risk of many serious health problems. For instance, there are ~3300 accidents per annum caused by NaOCl solutions in Britain. In addition, the National Fire Protection Agency (NFPA) has declared that solutions containing more than 40% NaOCl by weight are considered as hazardous oxidizers. Moreover, NaOCl is an expensive chemical substance and a concentration of 40 g/L is required to remove the dissolved H_2S (at 20 mg/L concentration) in wastewater [12]. From that, chemical scrubbing in packed towers is costly [13]. Oxidation reactions are generally corrosive and the mixing of an acid cleaner with a NaOCl bleach generates chlorine gas. Also, the mixtures of other cleaning agents and organic matter would lead to a gaseous reaction causing acute lung injury. Occupational Safety and Health Administration (OSHA) has also warned that long term exposure to NaOCl would cause serious health problems.

Owing to the shortcomings of chemical adsorbents, the use of non–conventional adsorbents consisting of agricultural wastes has recently been proposed. Fine Rubber Particle Media (FRPM) has limited porosity and hence its surface area is inadequate to support the pure physical adsorption of H_2S with the carbonated steel slag [14, 15]. On the other hand, the use of crushed oyster shell as adsorbent has been examined by Asaoka et al. [16]. The removal of Mn and H_2S from palm oil mill effluent (POME) using activated carbon was studied [17, 18]. In the current work, it has been found that eggshells, consisting of 94%–97% calcium carbonate, can be regarded as a practical adsorbent because it is easily available and cost–effective.

Huge amounts of eggshells are produced as a by–product because hen's eggs are one of most common traditional food articles and are utilized universally. Eggshells occupy ~11% of the total weight of an egg [19, 20] and they are normally thrown away without any pre–treatment [21], which leads to environmental pollution such as odor. Recently eggshells have been found to contain a high amount of minerals and amino acids [21], and exhibit interesting characteristics such as high porosity, good antibacterial or anti–inflammatory behavior [20], and excellent adsorbent properties [22]. Eggshells membranes have been applied in areas such as therapeutic, nutraceutical, metallurgy, and bioremediation areas [20]. In addition, eggshells have been used to remove heavy metals (21–160 mg/g) [23], phenolic compounds (0.052–0.143 dm^3/mg) [24], dyes (113.6 mg/g) [22] and pesticides (0.964 mmol/g) [25]. From the mentioned adsorption capacities, it is clear that eggshell–derived materials have a high ability to absorb the different materials with high efficiency.

In addition, due to properties such as high amounts of minerals and amino acids [21]; high porosity, antibacterial or anti–inflammatory characteristics [20], and excellent adsorbent properties [22], researchers have shifted their focus onto natural porous materials in the last couple of years. Various researches have been conducted to evaluate the adsorption ability of eggshell as a low cost adsorbent, in artificial wastewater with mono– or multi–components. Researchers have demonstrated the effectiveness of this adsorbent in the removal of heavy metals [23]

This study aims to evaluate the adsorption capacity of calcite eggshells while removing the dissolved H_2S in wastewater (from petroleum industry). In addition, a suitable kinetic and equilibrium isotherm model was identified in order to describe the current adsorption process employed using eggshells.

2. MATERIALS AND METHODS

2.1 Preparation of the Adsorbent

The eggshells were collected from poultry dump sites and they were immediately washed with deionized water to remove impurities. To dissolve the residual shells, the inner membrane was dismantled from the main eggshells and soaked in an acetic acid solution (70%) for two days, then washed with deionized water to reduce the acidity level up to a neutral pH. The eggshells were then blended, permeated through a set of sieves to 0.25, 0.3 and 0.5 mm, and finally dried at 105 °C in a hot air oven for eight hours. The eggshells were then calcinated at a temperature of 900 °C for 2 h soaking time, which was carried out at a constant heating rate of 10 °C/min with nitrogen (N_2) flow rate of 30 cm^3/min. The pyrolysis treatments were conducted in a horizontal furnace.

2.2 Physical and Chemical Characterization Measurements

The porous texture and morphology were examined by scanning electron microscope (SEM). The porous properties of the resulting eggshell particles were investigated by measurement of the nitrogen adsorption–desorption isotherm. The SEM runs at 20 kV accelerating potential on a HITACHI S–3400N. In order to measure the pH of surface adsorbent, a sample consisting of 0.4 g of dry carbon powder was added into 20 ml of water. The suspension was stirred overnight to reach equilibrium and subsequently the pH of the suspension was measured. Fourier transform infrared (FTIR) was used to examine the functional groups (responsible for H_2S adsorption) on the surfaces of modified and unmodified samples.

2.3 Preparation of Hydrogen Sulfide Solution

In this work, the synthesis of wastewater was prepared using the standard laboratory reaction process between hydrochloric acid (HCl) and ferrous sulfide (FeS) in a Kipp generator to produce H_2S, which was then allowed to dissolve in distilled water according to the following reaction:

$$FeS\ (s) + 2HCl\ (aq) \rightarrow FeCl_2\ (aq) + H_2S\ (g) \tag{1}$$

2.4 Batch Equilibrium Studies

The adsorption behaviors of unmodified eggshell particles were determined by examining the rate of removal of H_2S dissolved in an aqueous solution. The pollutant concentration was initially measured. All the experiments were performed using a batch process. The adsorption was carried out under a fume hood due to the toxicity of H_2S. A sample of 0.1g of calcite of eggshells was used. The solution pH was fixed to ~7.0 (neutral), and the solution was shaken at 150 rpm at 30 °C for 14 hours to determine the adsorption capacity. A spectrophotometer (HACH DR2800) was used to measure the residual solution after filtered the suspensions. Eq. (2) was used to calculate the adsorption capacity of the pollutants [26, 27].

$$q_e = \frac{(C_0 - C_e)V}{m} \tag{2}$$

where V is the solution volume (L), m is the mass of the adsorbent (g), C_o and C_e are the initial and final concentrations of the pollutant, respectively, and q_e is adsorption capacity (mg/g). In order to ensure the repeatability of the experimental result, all adsorption experiments were repeated for three times and it was found that the maximum deviation was within 5%. Subsequently, the equilibrium data were fitted using isotherm models.

2.5 Adsorption Isotherm Models

In the current study, the correlation between the adsorbent and the adsorbate at equilibrium is described using four well–known isotherm models, namely Langmuir, Freundlich, Temkin and Dubinin–Radushkevich models [28]. The parameters such as isotherm constants, Sum of Squared Error (SSE), and fitting (R^2) were subsequently determined.

2.5.1 Langmuir Isotherm

Langmuir isotherm assumes that adsorption takes place at a specific surface which contains a finite number of adsorption sites. This process is commonly known as homogeneous adsorption, whereby constant enthalpy and sorption activation energy are extracted from each molecule [29, 30]. The linear form of Langmuir's isotherm model can be expressed as:

$$\frac{C_e}{q_e} = \frac{1}{Q_0\, b} + \left(\frac{1}{Q_0}\right) C_e \tag{3}$$

where C_e is the equilibrium concentration of the adsorbate (H_2S) (mg/L), Q_o and b are Langmuir constants, and q_e is the amount of adsorbate adsorbed per unit mass of adsorbent (mg/g). The main characteristics of the Langmuir isotherm can be expressed in terms of the dimensionless equilibrium parameter (R_L), which is defined by:

$$R_L = \frac{1}{1+bC_0} \tag{4}$$

where C_0 the initial concentration of H_2S (mg/L) and b is the Langmuir constant. According to [30], the value of RL indicates the shape of the isotherm to be either unfavorable (R_L > 1), favorable (0 < R_L < 1), linear (R_L = 1) or irreversible (R_L = 0).

2.5.2 Freundlich Isotherm

The Freundlich isotherm assumes heterogeneous surface energies and it becomes more heterogeneous as the value of the slope approaches zero [31]. The slope ranges between 0 and 1 and it is used to measure the adsorption intensity or surface heterogeneity. The slope (*1/n*) value of >1 indicates cooperative adsorption [32]. The correlation coefficient (R^2) indicates the fitting error. Equation (5) gives the linear Freundlich model:

$$\log q_e = \log K_F + \left({}^{1}/_{n}\right) \log C_e \tag{5}$$

where q_e is the adsorption capacity at equilibrium (mg/g), C_e is the equilibrium concentration of the adsorbate (H_2S) and K_F and n are Freundlich constants.

2.5.3 Temkin Isotherm Model

Temkin isotherm assumes indirect interactions between the adsorbent and the adsorbate molecules on adsorption isotherms. The heat of adsorption of all the molecules in the layer would decrease linearly (instead of logarithmically) due to the interactions [33, 34]. The Temkin isotherm is examined using Eq. (6):

$$q_e = \frac{RT}{b} lnA_T + \left(\frac{RT}{b_T}\right) lnC_e \tag{6}$$

where $RT/b = B$, R is the gas constant (8.314 J/mol K) and T is the absolute temperature in K, and b is related to the heat of adsorption (J/mol).

2.5.4 Dubinin–Radushkevich Isotherm

Dubinin and Radushkevich isotherm model is generally applied to express the adsorption mechanism on the heterogeneous surface. Based on the potential theory [35].

$$lnq_e = lnq_d - K_{ad}\varepsilon^2 \tag{7}$$

where ε can be correlated as:

$$\varepsilon = RTln\,[1 + \frac{1}{C_e}] \tag{8}$$

Here, q_d is the adsorption capacity (mg/g).

2.6 Kinetic Studies

Adsorption kinetics models can be used to simulate the uptake of H_2S by adsorbents. In order to investigate the adsorption kinetics of H_2S onto the adsorbents, two well–known kinetic models, i.e. the pseudo–first–order and the pseudo–second–order models, are implemented.

2.6.1 Pseudo–first–order Kinetic Model

The rate constant of adsorption is determined from the pseudo–first–order Eq. given by Langergren and Svenska [27, 36]:

$$\ln(q_e - q_t) = \ln q_e - k_1\, t, \tag{9}$$

where q_e and q_t are the amounts of dissolved H_2S (mg/g) at equilibrium and at time t(h), respectively, and $k1$ is the rate constant of adsorption (h^{-1}). $k1$ is calculated from the linear plot of Eq. (9).

2.6.2 Pseudo–second–order Kinetic Model

A pseudo–second–order Eq. based on equilibrium adsorption [34, 37] is expressed as:

$$\frac{t}{q_t} = \frac{1}{k_2 q_e^2} + \frac{1}{q_2}\ t \tag{10}$$

where k_2 (g/mg h) is the rate constant of second–order adsorption.

2.6.3 Validity of Kinetic Model

Besides R^2, the Sum of Squared Error (SSE, %) is calculated for all kinetic models. The adsorption kinetics of H_2S of eggshells calcinations are tested at different initial concentrations. In general, SSE is expressed as:

$$SSE(\%) = \sqrt{\frac{\sum(q_{e,exp} - q_{e,cal})^2}{N}} \tag{11}$$

where N is the number of data points. q_{exp} and q_{cal} (mg/g) are the experimental and calculated adsorption capacities, respectively. The numerical fitting is good if R^2 is ~1.0 and SSE is ~ 0.0.

3. RESULTS AND DISCUSSION

3.1 Textural characterization of prepared adsorbent

The pyrolysis treatment of eggshells has a significant role to enhance the porosity and oxygenated functional group. During thermal treatment, the calcium carbonate ($CaCO_3$), converted to CaO and CO_2, is emitted as a by–product that might enhance the efficiency of the adsorbent toward H_2S [38] as described by Eq. (12). Scanning electron microscopy (SEM) and FTIR were used to characterize the modified and raw eggshells. The results obtained from SEM are shown in Fig. 1(a) and 1(b).

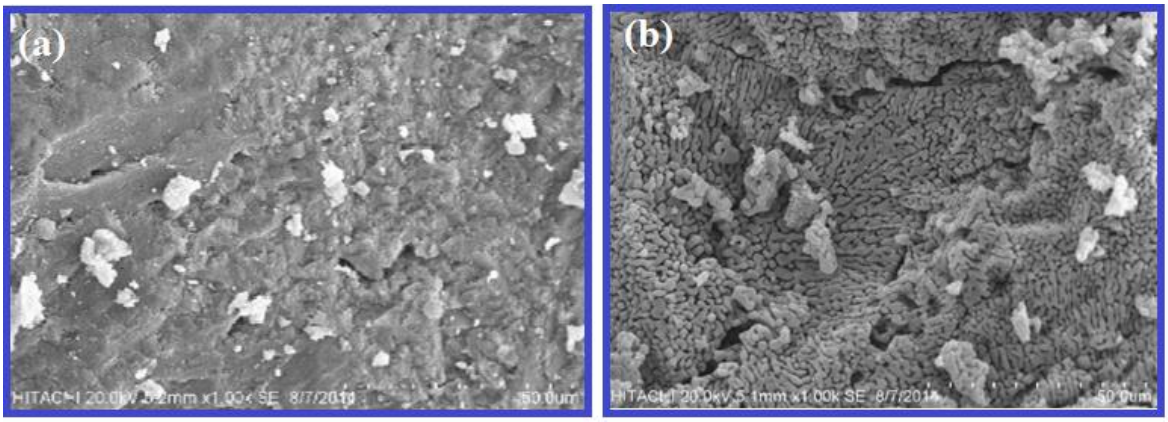

Fig. 1: SEM images of raw (a) and calcite (b) eggshells.

Figure 1(a) shows that raw eggshells exhibit low porosity, while enhanced porosity is observed for modified (calcinated) eggshells as illustrated in Fig. 1(b). From the eggshell calcination process, the (O_2) and (C) components have been reduced. The acidic medium and the high concentration of H^+ have increased the number of positively charged $CaOH^{2+}$.

Equation (13) shows the dissociation of calcium oxide in water to form calcium hydroxide on the surface of the adsorbent. Equation (14) shows the reaction of H_2S with calcium hydroxide. The OH^- from $Ca(OH)_2$ reacts with H_2S to form $Ca(HS)_2$, which is then converted to elemental sulfur (see Eq. (15).

$$CaCO_3 \rightarrow CaO + CO_2 \tag{12}$$

$$CaO + H_2O \rightarrow Ca(OH)_2 \tag{13}$$

$$Ca(OH)_2 + H_2S \rightarrow Ca(HS)_2 + 2H_2O \tag{14}$$

$$Ca(HS)_2 + O_2 \rightarrow Ca(OH)_2 + 2S \tag{15}$$

The FTIR method has been widely used to characterize the surface oxygenated groups of different oxides on the adsorbent surface. The FTIR structure of calcite eggshells exhibits an angular pattern of fracture as seen in Fig. 2. The bands of the modified adsorbent are located at 712, 882, 1080 and 1400 cm^{-1}, which corresponds to the presence of symmetric stretching υ1 mode of carbonate, out–of–plane bending (υ2 mode) vibrations of carbonate, υ1 and υ3 mode of crystalline vaterite ($CaCO_3$) phase. Decreasing the intensity of the former bands after calcination indicates to the conversion of calcium carbonate into calcium oxide. In addition the band at 3640 cm^{-1} is due to O–H of adsorbed water. Same observations noticed in studies done by others [39–41].

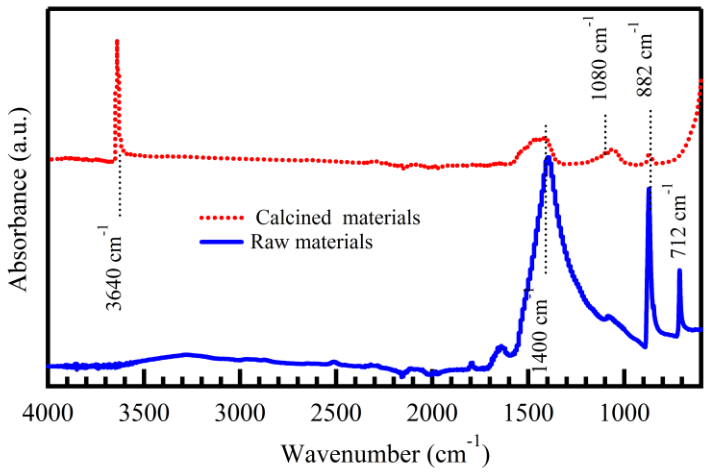

Fig. 2: FTIR of the calcite and raw materials of eggshells.

3.2 Effect of Contact Time and Initial H_2S Concentration on Adsorption Equilibrium

A series of contact time experiments for the H_2S adsorption process have been carried out at a temperature of 30 °C for different initial concentrations (100–500 mg/L) and the results are shown in Fig. 3. For cases of lower initial concentration (100–200 mg/L), a relatively short equilibrium time of ~6 hours is needed. However, cases of higher initial concentrations (300–500 mg/L) require a longer time (~9 hours) to reach equilibrium. The adsorption rate was initially high but it reached equilibrium after a sufficiently long period. This phenomenon occurs due to the abundance of vacant surface sites available for adsorption during the initial stage. After a long period of time, the remaining vacant surface sites are difficult to be occupied due to repulsive forces between the solute molecules on the solid and bulk phases. Therefore, the initial stage plays an important role during the adsorption process. At the equilibrium point, the amount of H_2S desorbing from the adsorbent is in a state of dynamic equilibrium with the amount of H_2S being adsorbed on the adsorbent. Choo [42] has reported that higher initial concentration could enhance the adsorption capacity, which is contradictory to that observed by Xiao [43].

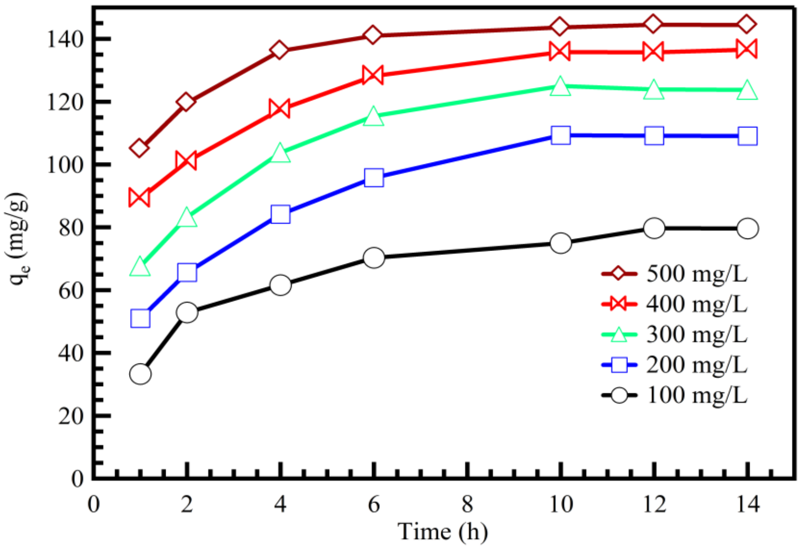

Fig. 3: The variation of adsorption capacity at various initial H_2S concentrations.

3.3 Adsorption Isotherms

The Langmuir, Freundlich, Temkin and Dubinin–Radushkevich isotherm models were applied to determine the suitable adsorption isotherm model for this process [44–47]. The isotherm models can also be used to demonstrate how the adsorption molecules are distributed between the solid phase and the liquid phase and to estimate the equilibrium time. The Langmuir adsorption isotherm equilibrium model for the adsorption process of H_2S onto calcite eggshells is shown in Fig. 4. The fitting error can be judged by examining the R^2 value. The straight line with a slope of $1/Q_o$ is obtained from the plot C_e/q_e vs. C_e is shown in Fig. 4. From Eq. (2), the Langmuir constants b and Q_o and are calculated and the values are reported in Table 1. The R^2 value of 0.9907 shows that the current adsorption data correlates well with the Langmuir isotherm model. Meanwhile, the value of R_L is 0.0503, showing that the Langmuir isotherm is favorable.

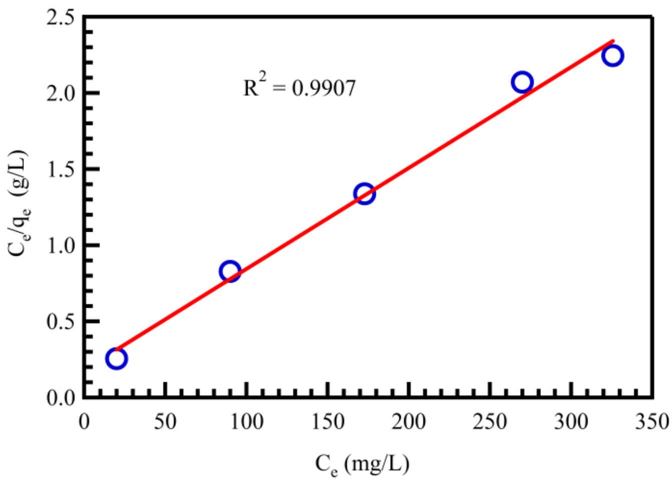

Fig. 4: Langmuir adsorption isotherm of H_2S onto eggshells adsorbent.

Table 1: Langmuir, Freundlich, Temkin and Dubinin–Radushkevich isotherm model parameters and correlation coefficients for adsorption of H_2S on the prepared adsorbent.

Isotherm models	**Concentration (mg/L)**	**Parameters**		**R^2**
Langmuir	500	Q_0 (mg/g)	*b* (l/mg)	0.9907
		150.07	0.0377	
Freundlich	500	K_F $(mg/g(L/mg)^{1/n}$	*1/n*	0.9825
		0.21515	0.2033	
Temkin	500	*A (L/g)*	b_T	0.9723
		1.886	115.5	
Dubinin–Radushkevich	500	q_d *(mg/g)*	K_{ad}	0.8483
		129.009	3.206×10^{-5}	

The numerical fitting using the Freundlich isotherm model is shown in Fig. 5. From the linear plot, the slope (1/*n*) is recorded at 0.2033. The fitting error is higher ($R^2 = 0.9825$) as compared to that of the Langmuir model. Accordingly, the Freundlich constants such as K_F and *n* are calculated from Eq. (8) and those values are listed in Table 1. For the Temkin isotherm model, q_e is plotted against $\ln(C_e)$ to obtain a straight line as shown in Fig. 6. The fitting error is higher than those of the Langmuir and Freundlich models. Finally, the Dubinin–Radushkevich isotherm model (see Fig. 7) reports the smallest R^2 value (0.8483).

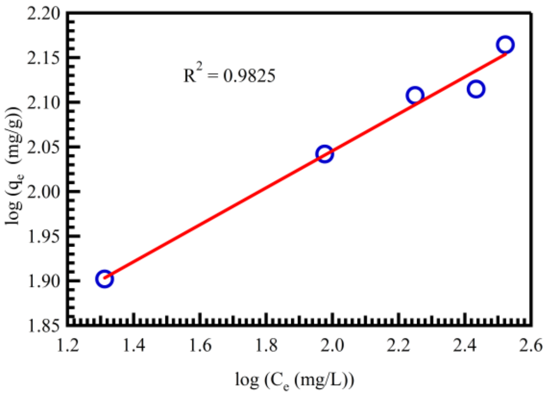

Fig. 5: Freundlich adsorption isotherm of H_2S onto eggshells adsorbent.

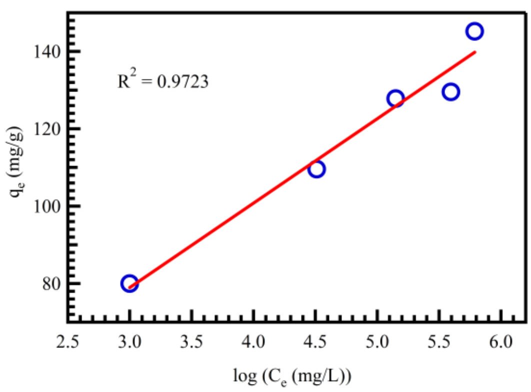

Fig. 6: Temkin adsorption isotherm of H_2S onto eggshells adsorbent.

3.5 Adsorption Kinetics

For the pseudo–first–order kinetic model shown in Fig. 8, the results of R^2 and *k*1 values are shown in Table 2. The R^2 values are low and the experimental q_e values are not in good agreement with those calculated from the pseudo–first–order kinetic model. This indicates that the pseudo–first–order equation may not be effective to describe the current adsorption process.

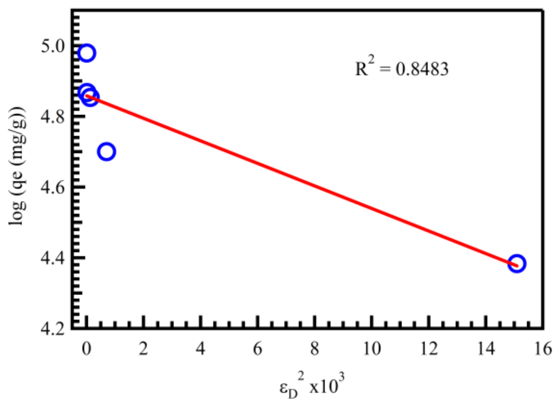

Fig. 7: Dubinin–Radushkevich adsorption isotherm of H_2S onto eggshells adsorbent.

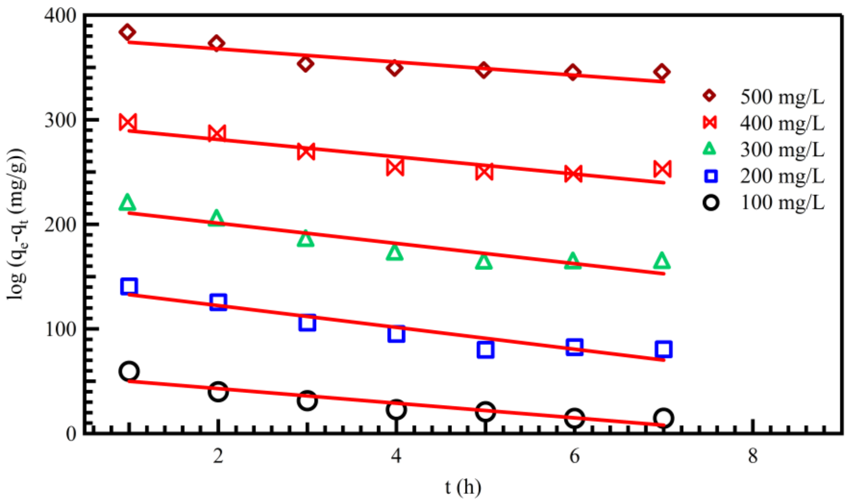

Fig. 8: Pseudo–first–order kinetics for adsorption of H_2S onto eggshells adsorbent.

Table 2: Pseudo–first–order, pseudo–second–order, intra–particle diffusion kinetic model and correlation coefficient for adsorption of H_2S onto eggshells adsorbent.

Initial H_2S concentration (mg/L)	**$q_{e,exp}$ (mg/g)**	**Pseudo–first–order kinetic model**				**Pseudo–second–order kinetic model**			
		$q_{e,cal}$ (mg/g)	**K_1 (1/ h)**	**R^2**	**SSE (%)**	**$q_{e,cal}$ (mg/g)**	**K_1 (1/ h)**	**R^2**	**SSE (%)**
100	80	59	7.4285	0.876	7.4	105	4.574	0.997	8.8
200	110	147.7	10.464	0.775	13.3	148	3.297	0.926	13.4
300	128	220	9.6785	0.744	32.52	153.3	4.940	0.991	9
400	130	298.4	8.3928	0.750	59.53	148.7	0.015	0.947	6.6
500	145	380	6.3571	0.704	83.08	157	0.012	0.998	4.2

However, when the pseudo–second–order kinetic model was used (Fig. 9), the correlation coefficients were greater than 0.926, showing that the adsorption of H_2S on calcite eggshells could be best described by the second–order kinetic model.

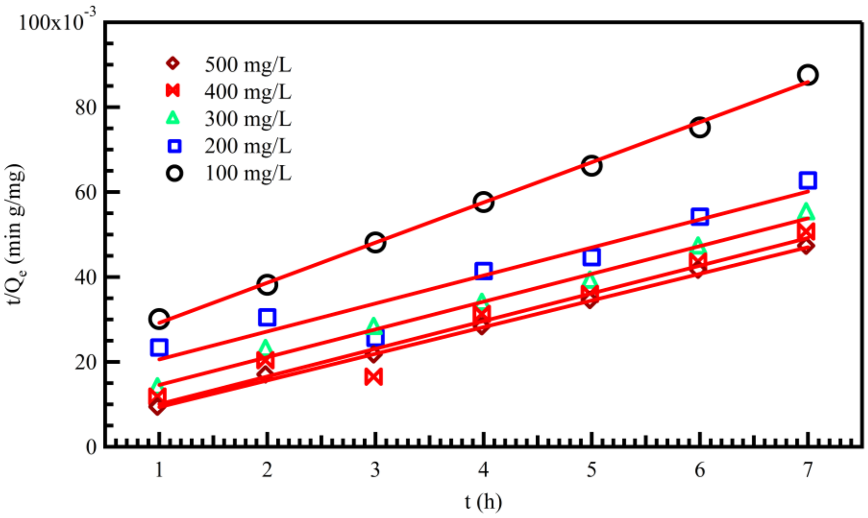

Fig. 9: Pseudo–second–order kinetics for adsorption of H_2S onto eggshells adsorbent.

4. CONCLUSIONS

In the current work, eggshells have been analyzed and characterized to determine their physical and chemical properties. The eggshells have been used for adsorption of H_2S dissolved in the synthetic wastewater. Adsorption of H_2S with an initial concentration of 100–500 mg/L has been examined with batch mode adsorption process. The optimum removal conditions were: 1 g/L, 6, 150 rpm and 14 h for dosage, pH, agitation speed and contact time. It has been found that the current adsorption behavior comes closer to the monolayer Langmuir isotherm model with R^2 values of 0.9907. With the kinetic data adapted to a pseudo second–order model gave R^2 value of 0.998 for the higher contaminant, the maximum adsorption capacity was found to be 150.07 mg/g. In general, the current work has witnessed the effectiveness of calcite eggshells for the removal of H_2S from wastewater over a wide range of initial concentrations.

ACKNOWLEDGEMENT

The authors would like to thank the Faculty of Chemical and Natural Resources Engineering, Universiti Malaysia Pahang, for the laboratory facilities provided to carry out this research.

REFERENCES

[1] Lambert TW, Goodwin VM, Stefani D, Strosher L. (2006) Hydrogen sulfide (H_2S) and sour gas effects on the eye. A historical perspective. Sci. Total Environ., 367(1):1–22.

[2] ATSDR, "Minimal Risk Levels (MRLs) for Hazardous Substances. Agency for Toxic Substances and Disease Registry.URL: http://www.atsdr.cdc.gov/mrls/," 2008.

[3] EPA, "Toxicological Review of Hydrogen Sulfide. URL: www.epa.gov/iris," 2003.

[4] Guidotti TL. (1994) Occupational exposure to hydrogen sulfide in the sour gas industry: some unresolved issues. Int. Arch. Occup. Environ. Health, 66(3):153–160.

[5] Hendrickson RG, Chang A, Hamilton RJ. (2004) Co-worker fatalities from hydrogen sulfide. Am. J. Ind. Med., 45(4):346–350.

[6] Heinonen A. (2012) Adsorption of hydrogen sulfide by modified cellulose nano/microcrystals.

[7] Silva PR, Ponte HA, Ponte MJJS, Kaminari NMS. (2011) Development of a new electrochemical methodology at carbon steel/Na_2S system for corrosion monitoring in oil refineries. J. Appl. Electrochem., 41(3):317–320.

[8] Ozekmekci M, Salkic G, Fellah MF. (2015) Use of zeolites for the removal of H2S: A mini-review. Fuel Process. Technol., 139:49–60.

[9] US Environmental Protection Agency. (1991) Hydrogen sulphide corrosion in wastewater collection and treatment system. in US Environmental Protection Agency, , p. Technical Report, 430/09-91-010.

[10] Chen Q, Wang J, Liu X, Li Z, Qiao W, Long D, Ling L. (2011) Structure-dependent catalytic oxidation of H2S over Na_2CO_3 impregnated carbon aerogels. Microporous Mesoporous Mater., 142(2–3):641–648.

[11] Derylo-Marczewska A. (1993) Analysis of the adsorption equilibrium for the system dilute aqueous solution of dissociating organic substance-activated carbon. Langmuir, 9(9):2344–2350.

[12] Tomar M, Abdullah THA. (1994) Evaluation of chemicals to control the generation of malodorous hydrogen sulfide in waste water. Water Res. 28(12):2545–2552.

[13] Couvert A, Sanchez C, Laplanche A, Renner C. (2008) Scrubbing intensification for sulphur and ammonia compounds removal. Chemosphere, 70(8):1510–1517.

[14] Wang N, Park J, Ellis TG. (2013) The mechanism of hydrogen sulfide adsorption on fine rubber particle media (FRPM). J. Hazard. Mater., 260:921–928.

[15] Asaoka S, Okamura H, Morisawa R, Murakami H, Fukushi K, Okajima T, Katayama M, Inada Y, Yogi C, Ohta T. (2013) Removal of hydrogen sulfide using carbonated steel slag. Chem. Eng. J., 228:843–849.

[16] Asaoka S, Yamamoto T, Kondo S, Hayakawa S. (2009) Removal of hydrogen sulfide using crushed oyster shell from pore water to remediate organically enriched coastal marine sediments. Bioresour. Technol., 100(18):4127–4132.

[17] Amosa MK. (2015) Process optimization of Mn and H_2S removals from POME using an enhanced empty fruit bunch (EFB)-based adsorbent produced by pyrolysis. Environ. Nanotechnology, Monit. Manag., 4:93–106.

[18] Amosa MK, Jami MS, AlKhatib MFR, Jimat DN, Muyibi SA. (2014) Comparative and optimization studies of adsorptive strengths of activated carbons produced from steam- and CO_2-activation for BPOME treatment. Adv. Environ. Biol., 8(3):603–612.

[19] Stadelman WJ. (2000) Eggs and egg products. In: Francis, F.J. (Ed.) Encyclopedia of Food Science and Technology, Second Ed.. John Wiley Sons, New York, p. 593–599.

[20] Pundir CS, Bhambi M, Chauhan NS. (2009) Chemical activation of egg shell membrane for covalent immobilization of enzymes and its evaluation as inert support in urinary oxalate determination. Talanta, 77(5):1688–1693.

[21] Tsai WT, Yang JM, Lai CW, Cheng YH, Lin CC, Yeh CW. (2006) Characterization and adsorption properties of eggshells and eggshell membrane.. Bioresour. Technol., 97(3):488–93.

[22] Tsai W-T, Hsien K-J, Hsu H-C, Lin C-M, Lin K-Y, Chiu C-H. (2008) Utilization of ground eggshell waste as an adsorbent for the removal of dyes from aqueous solution. Bioresour. Technol., 99(6):1623–1629.

[23] Chojnacka K. (2005) Biosorption of Cr (III) ions by eggshells. J. Hazard. Mater., 121(1):167–173.

[24] Koumanova B, Peeva P, Allen SJ, Gallagher KA, Healy MG. (2002) Biosorption from aqueous solutions by eggshell membranes and Rhizopus oryzae: equilibrium and kinetic studies. J. Chem. Technol. Biotechnol., 77(5):539–545.

[25] Elwakeel KZ, Yousif AM. (2010) adsorption of malathion on thermally treated egg shell material 2. Materials and methods. Water Sci. Technol., 61(4):53–65.

[26] Mohammad YS, Igboro SB, Giwa A, Okuofu CA. (2014) Modeling and optimization for production of rice husk activated carbon and adsorption of phenol. J. Eng. 2014: http://dx.doi.org/10.1155/2014/278075.

[27] Agarwal S, Sadegh H, Monajjemi M, Hamdy AS, Ali GAM, Memar AOH, Shahryari-Ghoshekandi R, Tyagi I, Gupta VK. (2016) Efficient removal of toxic bromothymol blue and methylene blue from wastewater by polyvinyl alcohol. J. Mol. Liq., 218:191-197.

[28] Allen SJ, Mckay G, Porter JF. (2004) Adsorption isotherm models for basic dye adsorption by peat in single and binary component systems. J. Colloid Interface Sci., 280(2):322–333.

[29] Weber TW, Chakravorti RK. (1974) Pore and solid diffusion models for fixed-bed adsorbers. AIChE J., 20(2):228–238.

[30] Bello OS, Adeogun IA, Ajaelu JC, Fehintola EO. (2008) Adsorption of methylene blue onto activated carbon derived from periwinkle shells: kinetics and equilibrium studies. Chem. Ecol., 24(4):285–295.

[31] Weber WJ, Physicochemical processes for water quality control. Wiley Interscience, 1972.

[32] Haghseresht F, Lu GQ. (1998) Adsorption characteristics of phenolic compounds onto coal-reject-derived adsorbents. Energy & Fuels, 12(6):1100–1107.

[33] Hosseini M, Mertens SFL, Ghorbani M, Arshadi MR. (2003) Asymmetrical Schiff bases as inhibitors of mild steel corrosion in sulphuric acid media. Mater. Chem. Phys., 78(3):800–808.

[34] Abdel Ghafar HH, Ali GAM, Fouad OA, Makhlouf SA. (2015) Enhancement of adsorption efficiency of methylene blue on Co_3O_4/SiO_2 nanocomposite. Desalin. Water Treat., 53:2980-2989.

[35] Günay A, Arslankaya E, Tosun I. (2007) Lead removal from aqueous solution by natural and pretreated clinoptilolite: adsorption equilibrium and kinetics. J. Hazard. Mater., 146(1):362–371.

[36] Lagergren S, Zur Theorie der sogenannten Absorption gelöster Stoffe. PA Norstedt & söner, 1898.

[37] Ho Y-S, McKay G. (1998) Sorption of dye from aqueous solution by peat. Chem. Eng. J., 70(2):115–124.

[38] Sanosh KP, Chu M-C, Balakrishnan A, Kim TN, Cho S-J. (2009) Utilization of biowaste eggshells to synthesize nanocrystalline hydroxyapatite powders. Mater. Lett., 63(24):2100–2102.

[39] Amosa MK, Jami MS, Alkhatib MFR. (2016) Electrostatic biosorption of COD, Mn and H_2S on EFB-based activated carbon produced through steam pyrolysis: an analysis based on surface chemistry, equilibria and kinetics. Waste and Biomass Valorization, 7(1):109–124.

[40] Alkhatib MF, Muyibi SA, Amode JO. (2011) Optimization of activated carbon production from empty fruit bunch fibers in one-step steam pyrolysis for cadmium removal from aqueous solution. Environmentalist, 31(4):349–357.

[41] Guo H, Sun P, Qin Z, Shan L, Zhang G, Cui S, Liang Y. (2014) Sodium lignosulfonate induced vaterite calcium carbonate with multilayered structure. Eur. J. Inorg. Chem., 2014(6):1001–1009.

[42] Choo HS, Lau LC, Mohamed A, Lee KT. (2013) Hydrogen sulfide adsorption by alkaline impregnated coconut shell activated carbon. J. Eng. Sci. Technol., 8(6):741–753.

[43] Xiao Y, Wang S, Wu D, Yuan Q. (2008) Catalytic oxidation of hydrogen sulfide over unmodified and impregnated activated carbon. Sep. Purif. Technol., 59(3):326–332.

[44] Habeeb OA, Ramesh K, Ali GAM, Yunus RM, Thanusha TK, Olalere OA. (2016) Modeling and optimization for H_2S adsorption from wastewater using coconut shell based activated carbon, Aust. J. Basic Appl. Sci. 10(17):136-147.

[45] Sadegh H, Ali GAM, Gupta VK, Makhlouf ASH, Shahryari-ghoshekandi R, Nadagouda MN, Sillanpää M, Megiel E. (2017) The role of nanomaterials as effective adsorbents and their applications in wastewater treatment, J. Nanostruct. Chem. 7(1):1-14.

[46] Gupta VK, Agarwal S, Sadegh H, Ali GAM, Bharti AK, Hamdy AS. (2017) Facile route synthesis of novel graphene oxide-β-cyclodextrin nanocomposite and its application as adsorbent for removal of toxic bisphenol A from the aqueous phase, J. Mol. Liq. http://doi.org/10.1016/j.molliq.2017.04.113.

[47] Amosa MK. (2016) Sorption of water alkalinity and hardness from high strength wastewater on bifunctional activated carbon: process optimization, kinetics and equilibrium studies, Environ. Technol., DOI: 10.1080/09593330.2016.1139631.